[88] Kenyon C, Chang J, Gensch E, Rudner A, Tabtiang R. A *C. elegans* mutant that lives twice as long as wild type. Nature 1993;366:461–4.
[89] Lee RY, Hench J, Ruvkun G. Regulation of *C. elegans* DAF-16 and its human ortholog FKHRL1 by the daf-2 insulin-like signaling pathway. Curr Biol 2001;11:1950–7.
[90] Lin K, Hsin H, Libina N, Kenyon C. Regulation of the *Caenorhabditis elegans* longevity protein DAF-16 by insulin/IGF-1 and germline signaling. Nat Genet 2001;28:139–45.
[91] Longo VD, Finch CE. Evolutionary medicine: from dwarf model systems to healthy centenarians? Science 2003;299:1342–6.
[92] Morris JZ, Tissenbaum HA, Ruvkun G. A phosphatidylinositol-3-OH kinase family member regulating longevity and diapause in *Caenorhabditis elegans*. Nature 1996;382:536–9.
[93] Ogg S, Paradis S, Gottlieb S, Patterson GI, Lee L, Tissenbaum HA, et al. The Fork head transcription factor DAF-16 transduces insulin-like metabolic and longevity signals in *C. elegans*. Nature 1997;389:994–9.
[94] Lin K, Dorman JB, Rodan A, Kenyon C. daf-16: an HNF-3/forkhead family member that can function to double the life-span of *Caenorhabditis elegans*. Science 1997;278:1319–22.
[95] Fabrizio P, Pozza F, Pletcher SD, Gendron CM, Longo VD. Regulation of longevity and stress resistance by Sch9 in yeast. Science 2001;292:288–90.
[96] Tatar M, Kopelman A, Epstein D, Tu MP, Yin CM, Garofalo RS. A mutant Drosophila insulin receptor homolog that extends life-span and impairs neuroendocrine function. Science 2001;292:107–10.
[97] Holzenberger M, Dupont J, Ducos B, Leneuve P, Geloen A, Even PC, et al. IGF-1 receptor regulates lifespan and resistance to oxidative stress in mice. Nature 2003;421:182–7.
[98] Bluher M, Kahn BB, Kahn CR. Extended longevity in mice lacking the insulin receptor in adipose tissue. Science 2003;299:572–4.
[99] Fabrizio P, Liou LL, Moy VN, Diaspro A, SelverstoneValentine J, Gralla EB, et al. SOD2 functions downstream of Sch9 to extend longevity in yeast. Genetics 2003;163:35–46.
[100] Honda Y, Honda S. The daf-2 gene network for longevity regulates oxidative stress resistance and Mn-superoxide dismutase gene expression in *Caenorhabditis elegans*. FASEB J 1999;13:1385–93.
[101] Murphy CT, McCarroll SA, Bargmann CI, Fraser A, Kamath RS, Ahringer J, et al. Genes that act downstream of DAF-16 to influence the lifespan of Caenorhabditis elegans. Nature 2003;424:277–83.
[102] Datta SR, Brunet A, Greenberg ME. Cellular survival: a play in three Akts. Genes Dev 1999;13:2905–27.
[103] Blume-Jensen P, Hunter T. Oncogenic kinase signalling. Nature 2001; 411:355–65.
[104] Testa JR, Bellacosa A. AKT plays a central role in tumorigenesis. Proc Natl Acad Sci USA 2001;98:10983–5.
[105] Cho H, Mu J, Kim JK, Thorvaldsen JL, Chu Q, Crenshaw III EB, et al. Insulin resistance and a diabetes mellitus-like syndrome in mice lacking the protein kinase Akt2 (PKB beta). Science 2001;292:1728–31.
[106] Vogel H, Lim DS, Karsenty G, Finegold M, Hasty P. Deletion of Ku86 causes early onset of senescence in mice. Proc Natl Acad Sci USA 1999;96:10770–5.
[107] de Boer J, Andressoo JO, de Wit J, Huijmans J, Beems RB, van Steeg H, et al. Premature aging in mice deficient in DNA repair and transcription. Science 2002;296:1276–9.
[108] Cao L, Li W, Kim S, Brodie SG, Deng CX. Senescence, aging, and malignant transformation mediated by p53 in mice lacking the Brca1 full-length isoform. Gene Dev 2003;17:201–13.
[109] Tyner SD, Venkatachalam S, Choi J, Jones S, Ghebranious N, Igelmann H, et al. p53 mutant mice that display early ageing-associated phenotypes. Nature 2002;415:45–53.
[110] Edelberg JM, Tang L, Hattori K, Lyden D, Rafii S. Young adult bone marrow-derived endothelial precursor cells restore aging-impaired cardiac angiogenic function. Circ Res 2002;90:E89–93.
[111] Rauscher FM, Goldschmidt-Clermont PJ, Davis BH, Wang T, Gregg D, Ramaswami P, et al. Aging, progenitor cell exhaustion, and atherosclerosis. Circulation 2003;108:457–63.
[112] Murasawa S, Llevadot J, Silver M, Isner JM, Losordo DW, Asahara T. Constitutive human telomerase reverse transcriptase expression enhances regenerative properties of endothelial progenitor cells. Circulation 2002;106:1133–9.

Angiotensin II Type 1a Receptor Is Involved in Cell Infiltration, Cytokine Production, and Neovascularization in Infarcted Myocardium

Haruhiro Toko, Yunzeng Zou, Tohru Minamino, Masaya Sakamoto, Masanori Sano, Mutsuo Harada, Toshio Nagai, Takeshi Sugaya, Fumio Terasaki, Yasushi Kitaura, Issei Komuro

Objective—Angiotensin II is critically involved in left ventricular remodeling after myocardial infarction. Neovascularization has been thought to prevent the development of left ventricular remodeling and deterioration to heart failure. To elucidate the role of angiotensin II in neovascularization during cardiac remodeling, we induced myocardial infarction in angiotensin II type1a receptor (AT1) knockout (KO) mice.

Methods and Results—There were more vessels in the border zone of infarcted hearts of wild-type (WT) mice and AT1KO mice at 14 days after operation, compared with in the left ventricle of sham-operated mice, and the number was larger in WT mice than in AT1KO mice. Consistent with these observations, the infarcted heart of AT1KO mice expressed lower levels of matrix metalloproteinase and endothelial nitric oxide synthase activity. More inflammatory cells such as granulocytes and macrophages were infiltrated in the infarcted hearts of WT mice than AT1KO mice at 4 days. A variety of cytokines and chemokines were increased in infarcted hearts of WT and AT1KO mice, and many of them were more remarkable in WT mice than in AT1KO mice at 14 days.

Conclusions—AT1 plays a critical role in inflammatory cell infiltration, cytokine production, and neovascularization in infarcted hearts. (***Arterioscler Thromb Vasc Biol.* 2004;24:664-670.**)

Key Words: angiotensin II ■ AT1 receptor ■ neovascularization ■ myocardial infarction ■ cardiac remodeling

Left ventricular remodeling after myocardial infarction (MI) causes progression of heart failure and death. The remodeling process is characterized by progressive expansion of the initial infarct area and dilation of the left ventricular lumen, with cardiomyocyte replacement by fibrous tissue deposition in the ventricular wall. Once these processes develop, the infarcted heart accelerates the deterioration of ventricular dysfunction, leading to heart failure.

See page 622

Accumulating evidence has suggested that the renin-angiotensin system (RAS) plays an important role in left ventricular remodeling after MI, and that inhibition of RAS with angiotensin-converting enzyme (ACE) inhibitors and angiotensin II (AngII) type 1a receptor (AT1) blockers suppresses the cardiac remodeling and reduces the mortality after MI in clinical studies and experimental models.[1–3] We also reported that AngII plays a critical role in cardiac remodeling and mortality after MI using AT1 knockout (KO) mice.[4] Although cardiac dysfunction was more prominent and mortality was higher in wild-type (WT) mice than AT1KO mice after MI,[4] the precise mechanism of how AngII induces left ventricular remodeling remains unknown.

It has been reported that neovascularization within the infarcted tissue is an integral component of the remodeling process and that induction of neovascularization reduces infracted area and mortality.[5] There are several controversial reports regarding the effects of AngII on vascularization. Some reports have shown that AngII induces neovascularization in tumors, ischemic legs, and retina,[6–8] but others have reported that inhibition of RAS stimulates neovascularization.[9] It has also been reported that an ACE inhibitor does not inhibit vascular growth during the early phase of post-infarcted cardiac remodeling and scar formation.[10] To elucidate the role of AngII in neovascularization in the heart, we induced MI and examined the number of vessels in AT1KO mice.

Methods

Animals

Eight-week-old male WT mice and AT1KO mice[11] from the same genetic background were used in the present study (SLC, Shizuoka,

Received December 22, 2003; revision accepted January 21, 2004.

From the Department of Cardiovascular Science and Medicine (H.T., Y.Z., T.M., M. Sakamoto, M. Sano, M.H., T.N., I.K.), Chiba University Graduate School of Medicine, Chiba, Japan; Discovery Laboratory (T.S.), Tanabe Seiyaku Co, Ltd, Osaka, Japan; and Third Department of Internal Medicine (F.T., Y.K.), Osaka Medical College, Osaka, Japan.

Correspondence to Dr Issei Komuro, Department of Cardiovascular Science and Medicine, Chiba University Graduate School of Medicine, 1-8-1 Inohana, Chuo-ku, Chiba 260-8670, Japan. E-mail komuro-tky@umin.ac.jp

© 2004 American Heart Association, Inc.

Arterioscler Thromb Vasc Biol. is available at http://www.atvbaha.org

DOI: 10.1161/01.ATV.0000122361.63827.ab

Japan). Mice were housed under climate-controlled conditions with a 12-hour light/dark cycle and were provided with standard food and water ad libitum as described previously.[12] All protocols were approved by the Institutional Animal Care and Use Committee of Chiba University.

MI Model

MI was produced in male WT and AT1KO mice by left coronary artery ligation as described previously.[4] Mice were sacrificed at 1, 4, 7, and 14 days after the operation. Sham-operated control mice did not receive coronary artery ligation. Before procedure, systolic blood pressure (SBP) and heart rate were measured by using a tail-cuff method.[12]

Hydralazine Treatment

It has been reported that SBP was lower in AT1KO mice than WT mice.[11,13] To examine the effect of BP on angiogenesis, we administered hydralazine (Norvartis Pharmaceuticals, Tokyo, Japan) to WT mice. WT mice were treated with hydralazine (3 mg/kg per day) through osmotic mini pump (Alzet, Palo Alto, Calif)[14] from 1 week before procedure to euthanization. Our preliminary experiments showed that SBP in WT mice treated with this dose of hydralazine was similar to that in AT1KO mice.

Number of Capillaries and Arterioles

We examined neovascularization by measuring the number of capillaries and arterioles in light microscopic sections taken from the border zone of the infarcted heart. Capillary endothelial cells and smooth muscle α-actin (SMA) were identified by immunohistochemical staining with anti-platelet/endothelial cell adhesion molecule (PECAM) antibody and anti-SMA antibody (PROGEN Biotechnik GmbH, Heidelberg, Germany), respectively. Ten random microscopic fields were examined and the number of capillaries and arterioles were expressed as the number of PECAM-positive capillaries and SMA-positive arteriole/high-power field (HPF) (×400).[7]

Histological Analysis for Inflammatory Response

Immunohistochemical analysis was performed with anti-Ly6G antibody, anti-Mac3 antibody, and anti-CD3 antibody (BD Pharmingen, San Diego, Calif) to detect granulocytes, macrophages, and T lymphocytes, respectively, according to the supplier's instructions. We counted positive cells in 10 random microscopic HPFs.

Western Blot Analysis

Protein extracts were obtained after homogenization of infarcted myocardium; 100 μg of protein was separated on a polyacrylamide gel and electroblotted onto nitrocellulose transfer membrane (Schleicher & Schuell, Dassel, Germany). The membrane was blocked with 5% skim milk and 0.5% BSA in PBS with 0.1% Tween-20 (T-PBS) and then probed with anti-matrix metalloproteinase (MMP)-2 antibody, anti- MMP-9 antibody, anti-Akt antibody, anti-endothelial nitric oxide synthase (eNOS) antibody, and anti-phospho-Akt antibody (Cell Signaling, Beverly, Mass) for 1 hour at room temperature. After incubation with the primary antibody, the membrane was washed in T-PBS and was incubated for 1 hour with peroxidase-conjugated secondary antibody. The reaction was detected using ECL detection reagent kit (Amersham Pharmacia, Buckinghamshire, UK).

NOS Activity Assay and NOS Inhibition

The NOS activity (calcium-dependent) in infarcted myocardium was examined using NOS assay kit (Calbiochem, San Diego, Calif) according to the manufacture's instruction. To examine the role of eNOS in angiogenesis after MI, we administered a NOS inhibitor, N^G-nitro-L-arginine methyl ester (L-NAME) (4 mg/kg per day) via drinking water to WT mice from 1 week before procedure to euthanization.

Ribonuclease Protection Assay

Total RNA was extracted from left ventricles with RNAzol B (Biotecx Laboratories) and analyzed by ribonuclease protection assay. Multi-probes template sets, mCK-3b and mCK-5, were available with reagents of in vitro transcription and ribonuclease protection assay (RiboQuant; Pharmingen). For all hybridization assays, we used 2 μg total RNA from the sham-operated mice hearts and the MI hearts.

Implantation of Sarcoma Cells

S180 sarcoma was inoculated subcutaneously into the right axilla of male WT and AT1KO mice at a dose of 2×10^6 cells in 0.2 mL PBS/mouse.[15] The mice were euthanized on day 14, and the tumor was removed and weighted. The number of capillaries in the tumor was counted as described.

Statistical Analysis

Data were shown as mean±SEM. Multiple group comparison was performed by one-way ANOVA followed by the Bonferroni procedure for comparison of means. Comparison between 2 groups was analyzed by the two-tailed Student t test or two-way ANOVA. Values of $P<0.05$ were considered statistically significant.

Results

AT1 Plays a Critical Role in Neovascularization After MI

We have previously reported that an infarcted size was significantly reduced in AT1KO mice compared with WT mice.[4] We therefore examined whether AT1 was involved in angiogenesis during the remodeling process. Immunohistochemical studies using anti-PECAM antibody revealed that the number of capillaries was increased in the border zone of the infarcted hearts of WT and AT1KO mice 14 days after MI as compared with hearts of sham-operated mice (Figure 1A), and this increase was more prominent in WT mice than in AT1KO mice (Figure 1A and 1B). Immunohistochemical analysis using anti-SMA antibody showed that the number of arteriole was also increased in the border zone of the infarcted hearts of WT mice on day 14 after MI, but not of AT1KO mice (Figure 1C and 1D). These results suggest that AT1 has stimulating effects on neovascularization after MI.

There was no significant difference in the heart rate between WT mice and AT1KO mice, but SBP in AT1KO mice was lower than that in WT mice (Figure 1E), which might affect neovascularization. To examine the effect of BP on angiogenesis after MI, we administered hydralazine to WT mice. SBP in WT mice treated with hydralazine was as low as that in AT1KO mice (Figure 1E). There was no significant difference in the capillary density between WT mice with hydralazine and WT mice without the treatment (Figure 1F). These results indicate that lower BP of AT1KO did not account for decreased angiogenesis in ischemic myocardium.

AT1 Mediates Cell Infiltration After MI

Because it has been reported that inflammation is an important trigger for ischemia-induced neovascularization[16] and that the RAS plays an important role in inflammatory responses,[17] we examined infiltration of inflammatory cells in the heart after MI. The numbers of granulocytes, macrophages, and T lymphocytes were examined in the myocardium on day 4 after MI using anti-Ly6G, anti-Mac3, and anti-CD3 antibodies, respectively. Many granulocytes (Figure 2A and 2D), macrophages (Figure

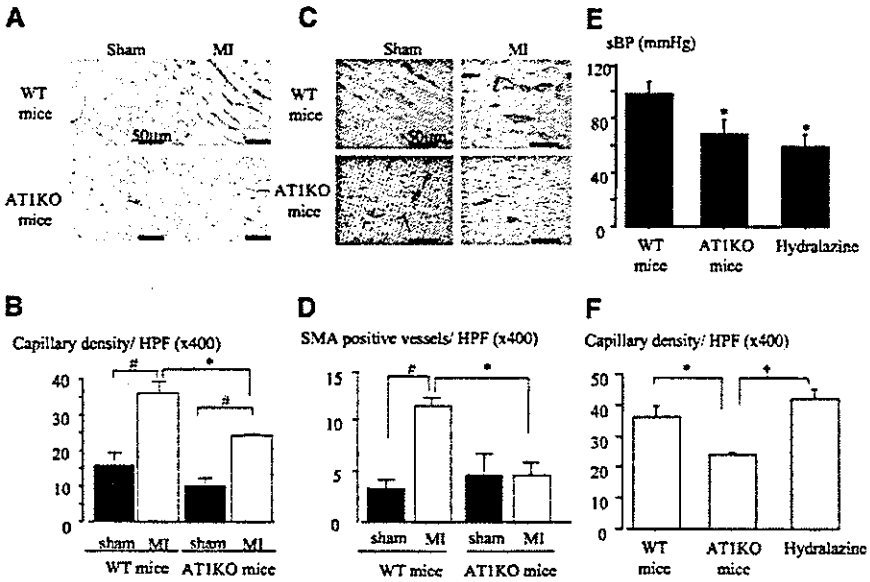

Figure 1. Neovascularization at 14 days after MI. A, The border zone of infarcted heart was stained with anti-PECAM antibody. B, Number of PECAM-positive capillaries per HPF. C, The border zone of infarcted heart was stained with anti-SMA antibody. D, Number of SMA-positive arterioles per HPF. E, Systolic blood pressure (SBP) before MI. F, Number of PECAM-positive capillaries per HPF. MI indicates myocardial infarction; WT, wild-type; AT1KO, angiotensin type1a receptor knockout; hydralazine, WT mice treated with hydralazine; HPF, high-power field. *$P<0.01$ versus WT, #$P<0.01$ versus sham, †$P<0.01$ versus AT1KO.

2B and 2E), and T lymphocytes (Figure 2C and 2F) were observed in the heart of WT and AT1KO mice after MI. The numbers of infiltrative cells such as granulocytes and macrophages were much larger in WT mice than those in AT1KO mice (Figure 2G), suggesting that AT1 is critically involved in cell infiltration in the myocardium after MI.

AT1 Induces MMPs and Activates Akt-1

Because it has been reported that MMPs are important for cell invasion into extravascular space[8] and that MMPs play a critical role in vascularization,[18] we next examined protein levels of MMP-2 and MMP-9 in the heart after MI. MMP-2 was increased on day 1 after MI in both WT mice and AT1KO mice (Figure 3A and 3B). MMP-9 was increased from day 4 in both WT mice and AT1KO mice (Figure 3A and 3C). The increases of MMP-2 and MMP-9 were more remarkable in WT mice compared with AT1KO mice (Figure 3B and 3C).

We examined another angiogenic factor, Akt-1.[19] The protein level of Akt-1 was increased in WT mice and AT1KO mice after MI (Figure 3D), and the increase was more prominent in WT mice (Figure 3E). The level of phosphorylated Akt-1 was more markedly increased after MI in WT mice than in AT1KO mice (Figure 3D and 3F), suggesting that AngII enhances activation of Akt-1 after MI.

Activation of eNOS by AngII Induces Angiogenesis

Akt has been shown to phosphorylate and activate eNOS,[20,21] thereby promoting angiogenesis.[22,23] We therefore examined the protein level and activity of NOS in the heart after MI. There was no significant change in eNOS protein levels after MI between WT mice and AT1KO mice (Figure 4A and 4B), but the NOS activity in WT mice was higher than that in AT1KO mice (Figure 4C). Expression of vascular endothelial growth factor after MI did not differ between WT mice and AT1KO mice (data not shown).

To further elucidate the role of eNOS activity in infarcted myocardium, we administered L-NAME to WT mice to reduce NO production. Treatment with L-NAME partially but significantly reduced the capillary density in the infarcted heart of WT mice (Figure 4D). In contrast, inhibition of NO production had no effect on neovascularization after MI in AT1KO mice. These results suggest that AngII-induced eNOS activation partly regulates angiogenesis after MI.

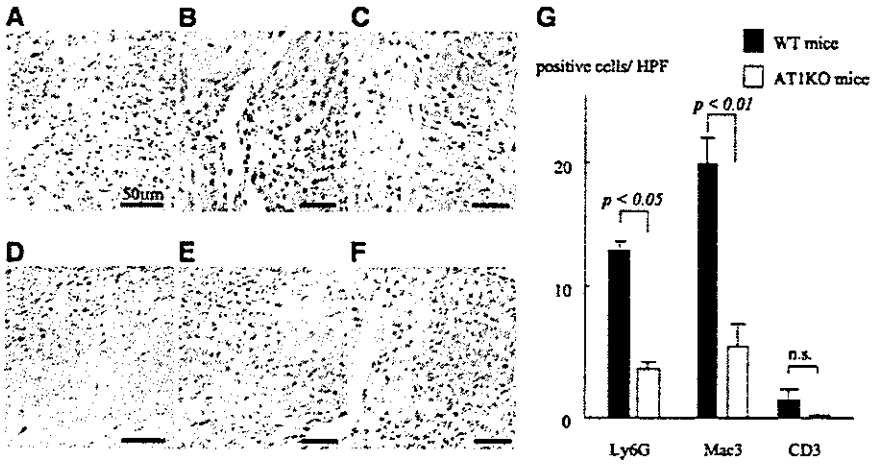

Figure 2. Cell infiltration in the myocardium at 4 days after MI. The immunohistochemical study using anti-Ly6G (granulocytes, A and D), anti-Mac3 (macrophages, B and E), and anti-CD3 (T cells, C and F) antibodies in WT mice (A, B, and C) and AT1KO mice (D, E and F). G, The number of infiltrating cells in the border zone of infarcted myocardium. Left columns show the number of Ly6G-positive cells, middle columns show the number of Mac3-positive cells, and right columns show the number of CD3-positive cells.

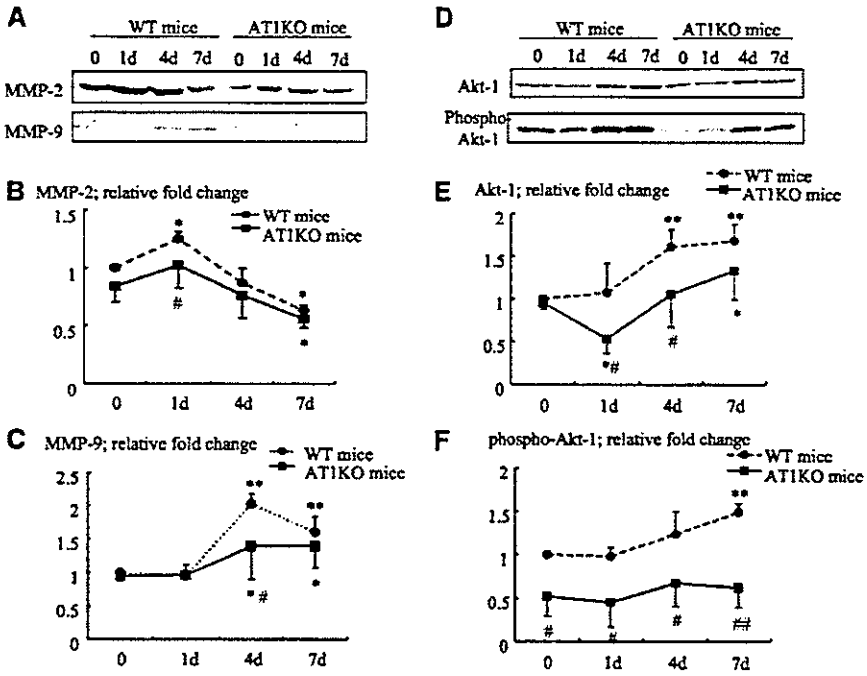

Figure 3. Protein levels of MMP-2, MMP-9, Akt-1, and phospho-Akt-1. A, Western blot analysis of MMP-2 and MMP-9 on days 0 (sham), 1, 4, and 7 after MI in WT mice and AT1KO mice. B, Relative fold change of MMP-2 protein levels. C, Relative fold change of MMP-9 protein levels. D, Western blot analysis of Akt-1 and phospho-Akt-1 on days 0 (sham), 1, 4, and 7 after MI in WT and AT1KO mice. E, Relative fold change of Akt-1 protein levels. F, Relative fold change of pospho-Akt-1 protein levels. $^{*}P<0.05$ and $^{**}P<0.01$ versus WT mice or AT1KO mice on day 0, $\#P<0.05$ and $\#\#P<0.01$ versus WT mice on the same day.

AT1 Is Involved in Induction of Cytokines and Chemokines in Infarcted Myocardium

Various cytokines and chemokines have been reported to play a critical role in left ventricular remodeling after MI.[24] We examined various cytokines and chemokines using ribonuclease protection assay. The expression levels of tumor necrosis factor-α, interleukin (IL)-6, transforming growth factor (TGF)-β1, TGF-β2, TGF-β3, interferon-inducible protein-10 (IP-10), monocyte chemoattractant protein-1 (MCP-1), exotoxin, RANTES, macrophage inflammatory protein (MIP)-α, MIP-1β, and MIP-2 were increased in infarcted myocardium in WT and AT1KO mice (Figure 5A and data not shown). Most of these cytokines and chemokines such as TGF-β1, TGF-β2, TGF-β3, IP-10, MCP-1, MIP-1α, MIP-1β, and MIP-2 were more strongly upregulated in WT mice compared with AT1KO mice (Figure 5B and data not shown).

Tumor Progression Is Inhibited in AT1KO Mice

Because tumor growth depends on angiogenesis,[25] we also investigated the role of AT1 in tumor angiogenesis. The tumor size in WT mice was larger than that in AT1KO mice 14 days after implantation of sarcoma cells (Figure 6A). The much more capillaries were observed in the tumor in WT mice compared with AT1KO mice (Figure 6B and 6C). These results indicate that AngII plays an important role in angiogenesis of tumors as well as ischemic hearts.

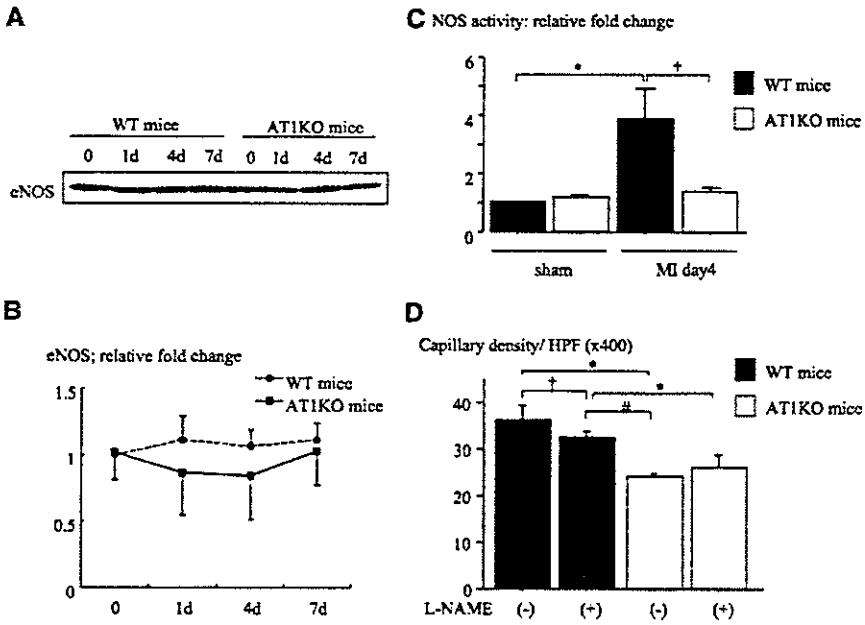

Figure 4. The effect of eNOS on angiogenesis after MI. A, Western blot analysis of eNOS on days 0 (sham), 1, 4, and 7 after MI in WT and AT1KO mice. B, Relative fold change of eNOS protein levels. C, Relative fold change of NOS activity on day 0 and day 4. $^{*}P<0.01$ versus sham, $\#P<0.05$ versus WT mice. D, Number of PECAM-positive capillaries per HPF on day 0 and day 14 after MI with or without L-NAME treatment. $^{*}P<0.01$, $\#P<0.01$, $\dagger P<0.05$.

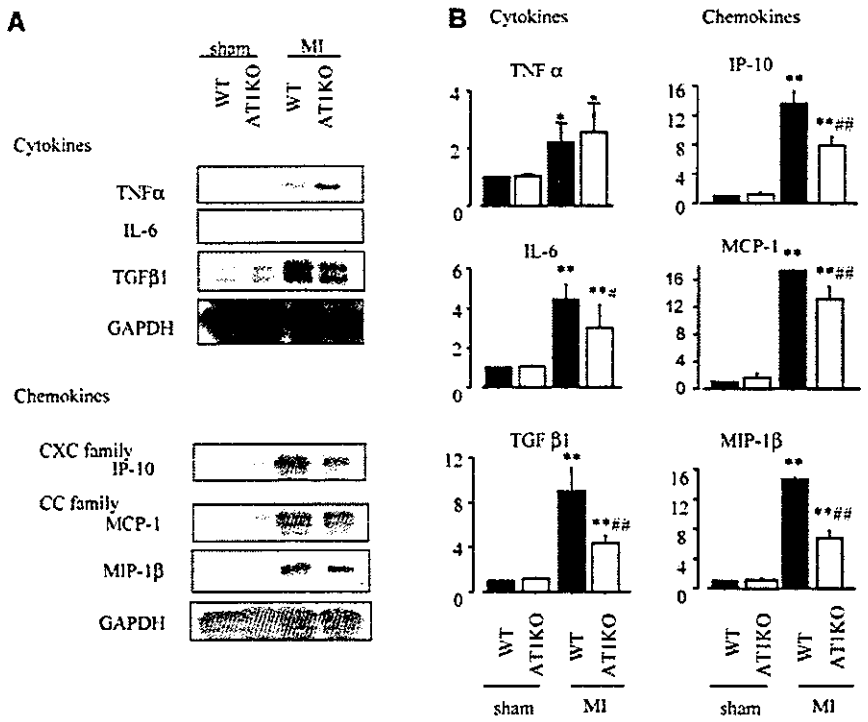

Figure 5. mRNA levels of cytokines and chemokines using RNase protection assay. A, mRNA level on day 0 (sham) and day 4 after MI in WT and AT1KO mice. B, Relative fold changes of mRNA levels. *$P<0.05$ and **$P<0.01$ versus sham, #$P<0.05$ and ##$P<0.01$ versus WT mice.

Discussion

AT1 Is Involved in Neovascularization After MI

It has been reported that an increase of neovascularization improves cardiac function and mortality,[5] and that inhibition of RAS is effective to prevent post-infarction cardiac remodeling.[1–4] It is unknown, however, whether activation of AngII/AT1 signaling induces or prevents vascularization in the infarcted heart. Some reports have demonstrated that AngII induces neovascularization in various experimental models including tumors, ischemic limb, retina, and chorioallantoic membrane.[6–8] To the contrary, there are some reports showing that inhibition of RAS induces neovascularization.[9] We thus examined in this study the role of AngII/AT1 in neovascularization during left ventricular remodeling and tumor progression using AT1KO mice. AT1KO mice exhibited less capillaries and arterioles than WT mice, suggesting that AT1 plays a pivotal role in neovascularization of the heart after MI and tumors.

AT1 Signal Plays an Important Role in Induction of MMPs and Cell Infiltration

To elucidate the molecular mechanism of how AngII induces neovascularization, we examined several molecules that have been reported to play an important role in angiogenesis. MMP-2 and MMP-9, gelatinases that digest basement membrane and play a critical role in cell invasion,[8] have been reported to be necessary for vascularization.[18,26] It has been reported that the treatment with ACE inhibitors decreases MMP-2 at mRNA and protein levels in vitro[27] and inhibits endothelial-cell migration by blocking the activity of MMP-2 and MMP-9.[26] In this study, protein levels of MMP-2 and MMP-9 were increased after MI and the increase was attenuated in AT1KO mice compared with WT mice. Histological examination revealed that infiltration of inflammatory cells such as granulocytes and macrophages was more remarkable in WT mice than AT1KO mice. These results and observations suggest that AngII induces transendothelial migration of inflammatory cells at least in part through enhanced production of MMP-2 and MMP-9. MMPs have been also demonstrated to contribute to tissue remodeling in a number of disease states, and inhibition of MMPs prevents left ventricular remodeling after MI.[28] Mice with targeted disruption of MMP-9 have attenuated ventricular remodeling and decreased cardiac rupture after infarction.[28] Our previous report also demonstrated that left ventricular dimension was

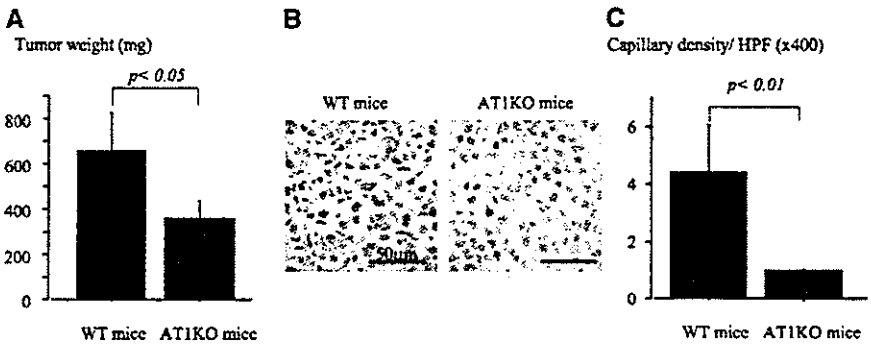

Figure 6. Tumor size and neovascularization at 14 days after sarcoma cell transplantation. A, Tumor size at 14 days after transplantation. B, The tumor was stained with anti-PECAM antibody. C, Number of PECAM-positive capillaries/HPF.

smaller in AT1KO mice than WT mice 4 weeks after MI.[4] These results suggest that MMPs activation via the AT1 signaling pathway is involved in neovascularization as well as in post-infarcted cardiac remodeling.

Activation of Akt-1 and eNOS by AngII Induces Angiogenesis in the Infarcted Myocardium

Akt plays an important role in cell survival, cell migration and angiogenesis.[29] AngII has been shown to activate Akt,[30] Akt phosphorylates, and eNOS,[20,21] thereby promoting angiogenesis. In this study, protein levels of Akt-1 were more increased in the heart of WT mice than AT1KO mice and Akt-1 was activated only in the heart of WT mice. Although there was no significant difference in protein levels of eNOS between WT mice and AT1KO mice, eNOS activity was significantly increased in WT mice compared with AT1KO mice. Moreover, the increase of capillaries in WT mice was partially inhibited by L-NAME treatment. These results suggest that AngII-induced activation of eNOS, mediated possibly by Akt, enhances angiogenesis in ischemic myocardium.

AngII Is Involved in the Production of Various Cytokines

The inflammation in cardiovascular diseases is associated with the activation of a variety of cells including lymphocytes, monocytes/macrophage, endothelial cells, smooth muscle cells, and cardiac myocytes, which express and secrete proinflammatory cytokines and chemokines.[24] These cytokines can modulate cardiac function and cardiovascular remodeling.[24] Various cytokines were increased after MI, and the increases of TGF-β, MIP-1, IP-10, and MCP-1 were more prominent in WT mice compared with AT1KO mice. These results suggest that AngII is involved in production of various cytokines after MI, which induce post-infarcted cardiac remodeling including impaired cardiac function and increased fibrosis.

Chemokines represent a family of inflammatory cytokines that induce chemotaxis of leukocyte subsets into inflammatory tissues.[31] CC-chemokines are potent chemoattractants and activators for monocytes and lymphocytes, whereas most CXC-chemokines attract neutrophils.[32] MCP-1 recruits monocytes, which produce proteolytic enzymes, reactive oxygen species, and inflammatory cytokines.[33] Recent studies have shown that neovascularization in response to tissue ischemia depends on macrophage infiltration[34] and that local infusion of MCP-1 markedly increases collateral and peripheral conductance in hindlimb ischemia model.[35] Moreover, inflammatory cytokines such as IL-1, IL-6–related cytokines, and MCP-1 have been reported to induce myocardial dysfunction[36,37] and cardiac remodeling through promotion of cardiomyocyte hypertrophy and apoptosis as well as alteration in extracellular matrix in the myocardium.[38] The MCP-1 overexpression mice showed hypertrophied left ventricular wall, dilated left ventricular dimension, and decreased cardiac function.[39] In this study, the MCP-1 expression was suppressed and the number of macrophage infiltrated into myocardium was less in AT1KO mice after MI compared with WT mice. These results and observations suggest that reduction of MCP-1 expression and macrophage infiltration might be related to less left ventricular remodeling despite less neovascularization in the heart of AT1KO mice.

AngII/AT1 signaling has 2 roles in left ventricular remodeling after MI. Activation of AT1 induces expression of chemokines and infiltration of inflammatory cells, which cause neovascularization possibly through enhanced expression of MMPs and activation of Akt. The enhanced neovascularization may prevent left ventricular remodeling by inhibition of cardiomyocyte apoptosis. However, AngII/AT1-induced cardiomyocyte hypertrophy, increased fibrosis, enhanced cytokines, and MMPs expressions induce left ventricular remodeling. Taken together with the previous reports,[4] inhibition of AngII/AT1 signal is important for preventing cardiac remodeling after MI, although it may suppress neovascularization.

Acknowledgments

We thank to E. Fujita, R. Kobayashi, A. Ohkubo, M. Watanabe, and M. Iida for technical assistant. This work was supported in part by grants from Japanese Ministry of Education, Science, Sports, and Culture and Japan Health Sciences Foundation, Takeda Medical Research Foundation, Uehara Memorial Foundation, grant-in-aid of The Japan Medical Association, The Kato Memorial Trust for Nambyo Research, and Takeda Science Foundation.

References

1. Effect of ramipril on mortality and morbidity of survivors of acute myocardial infarction with clinical evidence of heart failure. The Acute Infarction Ramipril Efficacy (AIRE) Study Investigators. *Lancet.* 1993; 342:821–828.
2. Latini R, Maggioni AP, Flather M, Sleight P, Tognoni G. ACE inhibitor use in patients with myocardial infarction. Summary of evidence from clinical trials. *Circulation.* 1995;92:3132–3137.
3. Pfeffer MA. ACE inhibition in acute myocardial infarction. *N Engl J Med.* 1995;332:118–120.
4. Harada K, Sugaya T, Murakami K, Yazaki Y, Komuro I. Angiotensin II type 1A receptor knockout mice display less left ventricular remodeling and improved survival after myocardial infarction. *Circulation.* 1999;100: 2093–2099.
5. Kocher AA, Schuster MD, Szabolcs MJ, Takuma S, Burkhoff D, Wang J, Homma S, Edwards NM, Itescu S. Neovascularization of ischemic myocardium by human bone-marrow-derived angioblasts prevents cardiomyocyte apoptosis, reduces remodeling and improves cardiac function. *Nat Med.* 2001;7:430–436.
6. Moravski CJ, Kelly DJ, Cooper ME, Gilbert RE, Bertram JF, Shahinfar S, Skinner SL, Wilkinson-Berka JL. Retinal neovascularization is prevented by blockade of the renin-angiotensin system. *Hypertension.* 2000; 36:1099–1104.
7. Sasaki K, Murohara T, Ikeda H, Sugaya T, Shimada T, Shintani S, Imaizumi T. Evidence for the importance of angiotensin II type 1 receptor in ischemia-induced angiogenesis. *J Clin Invest.* 2002;109:603–611.
8. Vu TH, Werb Z. Matrix metalloproteinases: effectors of development and normal physiology. *Genes Dev.* 2000;14:2123–2133.
9. Fabre JE, Rivard A, Magner M, Silver M, Isner JM. Tissue inhibition of angiotensin-converting enzyme activity stimulates angiogenesis in vivo. *Circulation.* 1999;99:3043–3049.
10. Kalkman EA, van Haren P, Saxena PR, Schoemaker RG. Early captopril prevents myocardial infarction-induced hypertrophy but not angiogenesis. *Eur J Pharmacol.* 1999;369:339–348.
11. Sugaya T, Nishimatsu S, Tanimoto K, Takimoto E, Yamagishi T, Imamura K, Goto S, Imaizumi K, Hisada Y, Otsuka A, Uchida H, Sugiura M, Fukuta K, Fukamizu A, Murakami K. Angiotensin II type 1a receptor-deficient mice with hypotension and hyperreninemia. *J Biol Chem.* 1995; 270:18719–18722.
12. Toko H, Zhu W, Takimoto E, Shiojima I, Hiroi Y, Zou Y, Oka T, Akazawa H, Mizukami M, Sakamoto M, Terasaki F, Kitaura Y, Takano H, Nagai T, Nagai R, Komuro I. Csx/Nkx2-5 is required for homeostasis and survival of cardiac myocytes in the adult heart. *J Biol Chem.* 2002; 277:24735–24743.

13. Harada K, Komuro I, Shiojima I, Hayashi D, Kudoh S, Mizuno T, Kijima K, Matsubara H, Sugaya T, Murakami K, Yazaki Y. Pressure overload induces cardiac hypertrophy in angiotensin II type 1A receptor knockout mice. *Circulation.* 1998;97:1952–1959.
14. Toko H, Oka T, Zou Y, Sakamoto M, Mizukami M, Sano M, Yamamoto R, Sugaya T, Komuro I. Angiotensin II type 1a receptor mediates doxorubicin-induced cardiomyopathy. *Hypertens Res.* 2002;25:597–603.
15. Wang G, Dong Z, Xu G, Yang Z, Shou C, Wang N, Liu T. The effect of antibody against vascular endothelial growth factor on tumor growth and metastasis. *J Cancer Res Clin Oncol.* 1998;124:615–620.
16. Salven P, Hattori K, Heissig B, Rafii S. Interleukin-1alpha promotes angiogenesis in vivo via VEGFR-2 pathway by inducing inflammatory cell VEGF synthesis and secretion. *FASEB J.* 2002;16:1471–1473.
17. Nicoletti A, Michel JB. Cardiac fibrosis and inflammation: interaction with hemodynamic and hormonal factors. *Cardiovasc Res.* 1999;41: 532–543.
18. Hiraoka N, Allen E, Apel IJ, Gyetko MR, Weiss SJ. Matrix metalloproteinases regulate neovascularization by acting as pericellular fibrinolysins. *Cell.* 1998;95:365–377.
19. Jiang BH, Zheng JZ, Aoki M, Vogt PK. Phosphatidylinositol 3-kinase signaling mediates angiogenesis and expression of vascular endothelial growth factor in endothelial cells. *Proc Natl Acad Sci U S A.* 2000;97: 1749–1753.
20. Dimmeler S, Fleming I, Fisslthaler B, Hermann C, Busse R, Zeiher AM. Activation of nitric oxide synthase in endothelial cells by Akt-dependent phosphorylation. *Nature.* 1999;399:601–605.
21. Fulton D, Gratton JP, McCabe TJ, Fontana J, Fujio Y, Walsh K, Franke TF, Papapetropoulos A, Sessa WC. Regulation of endothelium-derived nitric oxide production by the protein kinase Akt. *Nature.* 1999;399: 597–601.
22. Matsunaga T, Warltier DC, Weihrauch DW, Moniz M, Tessmer J, Chilian WM. Ischemia-induced coronary collateral growth is dependent on vascular endothelial growth factor and nitric oxide. *Circulation.* 2000; 102:3098–3103.
23. Murohara T, Asahara T, Silver M, Bauters C, Masuda H, Kalka C, Kearney M, Chen D, Symes JF, Fishman MC, Huang PL, Isner JM. Nitric oxide synthase modulates angiogenesis in response to tissue ischemia. *J Clin Invest.* 1998;101:2567–2578.
24. Frangogiannis NG, Smith CW, Entman ML. The inflammatory response in myocardial infarction. *Cardiovasc Res.* 2002;53:31–47.
25. Folkman J. Angiogenesis in cancer, vascular, rheumatoid and other disease. *Nat Med.* 1995;1:27–31.
26. Volpert OV, Ward WF, Lingen MW, Chesler L, Solt DB, Johnson MD, Molteni A, Polverini PJ, Bouck NP. Captopril inhibits angiogenesis and slows the growth of experimental tumors in rats. *J Clin Invest.* 1996;98: 671–679.
27. Prontera C, Mariani B, Rossi C, Poggi A, Rotilio D. Inhibition of gelatinase A (MMP-2) by batimastat and captopril reduces tumor growth and lung metastases in mice bearing Lewis lung carcinoma. *Int J Cancer.* 1999;81:761–766.
28. Heymans S, Luttun A, Nuyens D, Theilmeier G, Creemers E, Moons L, Dyspersin GD, Cleutjens JP, Shipley M, Angellilo A, Levi M, Nube O, Baker A, Keshet E, Lupu F, Herbert JM, Smits JF, Shapiro SD, Baes M, Borgers M, Collen D, Daemen MJ, Carmeliet P. Inhibition of plasminogen activators or matrix metalloproteinases prevents cardiac rupture but impairs therapeutic angiogenesis and causes cardiac failure. *Nat Med.* 1999;5:1135–1142.
29. Shiojima I, Walsh K. Role of Akt signaling in vascular homeostasis and angiogenesis. *Circ Res.* 2002;90:1243–1250.
30. Ushio-Fukai M, Alexander RW, Akers M, Yin Q, Fujio Y, Walsh K, Griendling KK. Reactive oxygen species mediate the activation of Akt/ protein kinase B by angiotensin II in vascular smooth muscle cells. *J Biol Chem.* 1999;274:22699–22704.
31. Taub DD, Oppenheim JJ. Chemokines, inflammation and the immune system. *Ther Immunol.* 1994;1:229–246.
32. Baggiolini M, Dewald B, Moser B. Interleukin-8 and related chemotactic cytokines–CXC and CC chemokines. *Adv Immunol.* 1994;55:97–179.
33. Ruiz-Ortega M, Bustos C, Hernandez-Presa MA, Lorenzo O, Plaza JJ, Egido J. Angiotensin II participates in mononuclear cell recruitment in experimental immune complex nephritis through nuclear factor-kappa B activation and monocyte chemoattractant protein-1 synthesis. *J Immunol.* 1998;161:430–439.
34. Polverini PJ, Cotran PS, Gimbrone MA, Jr., Unanue ER. Activated macrophages induce vascular proliferation. *Nature.* 1977;269:804–806.
35. Risau W. Mechanisms of angiogenesis. *Nature.* 1997;386:671–674.
36. Finkel MS, Oddis CV, Jacob TD, Watkins SC, Hattler BG, Simmons RL. Negative inotropic effects of cytokines on the heart mediated by nitric oxide. *Science.* 1992;257:387–389.
37. Yokoyama T, Vaca L, Rossen RD, Durante W, Hazarika P, Mann DL. Cellular basis for the negative inotropic effects of tumor necrosis factor-alpha in the adult mammalian heart. *J Clin Invest.* 1993;92: 2303–2312.
38. Bozkurt B, Kribbs SB, Clubb FJ, Jr., Michael LH, Didenko VV, Hornsby PJ, Seta Y, Oral H, Spinale FG, Mann DL. Pathophysiologically relevant concentrations of tumor necrosis factor-alpha promote progressive left ventricular dysfunction and remodeling in rats. *Circulation.* 1998;97: 1382–1391.
39. Kolattukudy PE, Quach T, Bergese S, Breckenridge S, Hensley J, Altschuld R, Gordillo G, Klenotic S, Orosz C, Parker-Thornburg J. Myocarditis induced by targeted expression of the MCP-1 gene in murine cardiac muscle. *Am J Pathol.* 1998;152:101–111.

The FASEB Journal express article 10.1096/fj.03-0637fje. Published online March 4, 2004.

Cytokine therapy prevents left ventricular remodeling and dysfunction after myocardial infarction through neovascularization

Masashi Ohtsuka,* Hiroyuki Takano,* Yunzeng Zou,* Haruhiro Toko,* Hiroshi Akazawa,* Yingjie Qin,* Masashi Suzuki,† Hiroshi Hasegawa,* Haruaki Nakaya,† and Issei Komuro*

*Department of Cardiovascular Science and Medicine and †Department of Pharmacology, Chiba University Graduate School of Medicine, 1-8-1 Inohana, Chuo-ku, Chiba 260-8670, Japan

Corresponding author: Issei Komuro, Department of Cardiovascular Science and Medicine, Chiba University Graduate School of Medicine. 1-8-1 Inohana, Chuo-ku, Chiba 260-8670, Japan. E-mail: komuro-tky@umin.ac.jp

ABSTRACT

Pretreatment with a combination of granulocyte colony-stimulating factor (G-CSF) and stem cell factor (SCF) has been reported to attenuate left ventricular (LV) remodeling after acute myocardial infarction (MI). We here examined whether the cytokine treatment started after MI has also beneficial effects. Anterior MI was created in the recipient mice whose bone marrow had been replaced with that of transgenic mice expressing enhanced green fluorescent protein (GFP). We categorized mice into five groups according to the following treatment: 1) saline; 2) administration of G-CSF and SCF from 5 days before MI through 3 days after; 3) administration of G-CSF and SCF for 5 days after MI; 4) administration of G-CSF alone for 5 days after MI; 5) administration of SCF alone for 5 days after MI. All the three treatment groups with G-CSF showed less LV remodeling and improved cardiac function and survival rate after MI. The number of capillaries, which express GFP, was increased and the number of apoptotic cells was decreased in the border area of all the treatment groups with G-CSF. Even if the cytokine treatment is started after MI, it could prevent LV remodeling and dysfunction after MI—at least in part—through an increase in neovascularization and a decrease in apoptosis in the border area.

Key words: apoptosis • bone marrow • G-CSF

It is important to prevent left ventricular (LV) remodeling after acute myocardial infarction (MI) because it causes heart failure and poor prognosis (1). After MI, many cardiomyocytes undergo cell death by the mechanisms of necrosis and apoptosis in the infarcted area, which is then replaced by fibrotic tissue. The infarcted area is gradually extended by the subsequent death of cardiomyocytes in the border area and expanded by abnormal wall tension (2). Myocardial ischemia plays a critical role in the cardiomyocyte death in the border area after MI and thus greatly affects LV remodeling (2). Recently, Orlic et al. have reported that a subset of bone marrow stem cells (BMSCs) differentiate into cardiomyocytes when injected into peri-infarcted area, which results in regeneration of the infarcted heart (3). They have also reported that a pretreatment with granulocyte colony-stimulating factor (G-CSF) and stem cell factor (SCF), which strongly induce mobilization of BMSCs from bone marrow (BM), attenuates LV remodeling after MI (4–6). Although these results suggest that the cytokine treatment is beneficial

to prevent LV remodeling, the cytokine treatment was started before MI and thus this protocol cannot be applied to humans. Furthermore, the molecular mechanism of how the cytokine treatment repairs the infarcted heart is not fully understood.

In the present study, we examined three points: 1) whether the cytokine treatment started after MI is as effective as the pretreatment; 2) whether the combination treatment with G-CSF and SCF is more effective than the single treatment with G-CSF alone or SCF alone; and 3) how G-CSF prevents LV remodeling and dysfunction after MI. We used mice that were replaced by BM cells of enhanced green fluorescent protein (GFP)-expressing mice to elucidate the role of BM cells in the reduction of infarct size.

MATERIALS AND METHODS

Murine MI model

C57BL/6 male mice at 12-weeks-old were used in this study. All protocols were approved by the Institutional Animal Care and Use Committee of Chiba University. Mice were anesthetized with pentobarbital and artificially ventilated with a respirator, and MI was produced by permanent ligation of the left coronary artery with a 10-0 nylon surgical suture under a dissecting microscope as previously described (7). Sham operation was performed by cutting pericardium.

Cytokine treatments

Mice were divided into the following five groups: 1) administration of vehicle (control, n=22); 2) administration of G-CSF (100 μg/kg/day, Kyowa Hakko Kogyo Co., LTD. Tokyo, Japan) and SCF (200 μg/kg/day, Kirin Brewery Co., LTD. Tokyo, Japan) from 5 days before MI through 3 days after (Pre-GS, n=16); 3) administration of G-CSF (100 μg/kg/day) and SCF (200 μg/kg/day) for 5 days after MI (Post-GS, n=20); 4) administration of G-CSF (100 μg/kg/day) alone for 5 days after MI (Post-G, n=20); 5) administration of SCF (200 μg/kg/day) alone for 5 days after MI (Post-S, n=21). We gave first injection of vehicle, G-CSF, or SCF at 2 h after MI subcutaneously (Fig. 1*A*). In addition, we added a sham-operated group (n=5) to clarify whether cytokine treatments act completely or partly on MI heart.

Physiological analysis

For physiological analysis, we examined hemodynamic parameters of the survived mice (Sham, n=5; Control, n=5; Pre-GS, n=10; Post-GS, n=16; Post-G, n=14; Post-S, n=9) at 2 weeks after MI by cardiac catheterization. Mice were anesthetized by intraperitoneal injection of a mixture of 100 mg/kg ketamine (Sigma Chemical Co., St. Louis, MO) and 5 mg/kg xylazine (Sigma). The right carotid artery was cannulated by Millar Mikro-Tip transducer (model SPR-612, Millar Instruments, Houston, TX) as described previously (8). Pressure signals were recorded by using MacLab 3.6/s data acquisition system (AD Instruments, Milford, MA) with sampling rate 2000 Hz. LV systolic pressure (LVP), LV end-diastolic pressure (LVEDP), and positive and negative first derivatives for maximal rates of LV pressure development (dP/dt and –dP/dt) were measured.

Histological analysis

We excised hearts (Sham, n=5; Control, n=5; Pre-GS, n=10; Post-GS, n=16; Post-G, n=14; Post-S, n=9) for histological analysis after catheterization. LV was fixed with 10% formalin overnight and dehydrated methanol and was embedded in paraffin. Serial sections at 4 μm were stained with hematoxylin-eosin and Azan-Mallory. The scar area was evaluated by tracing the blue area in Azan-Mallory staining. We evaluated LV remodeling as described previously (9).

Capillary density, inflammatory cells, and apoptotic cell death

We analyzed inflammatory cells, capillary density, and apoptotic cells by another series of experiment (Control, n=5; Pre-GS, n=5; Post-GS, n=5; Post-G, n=5). The capillaries in the border area of MI hearts were identified by staining endothelial cells with antibody against platelet/endothelial cell adhesion molecule-1(PECAM-1; Santa Cruz Biotechnology, Santa Cruz, CA; 10). The number of capillaries per square millimeter was counted in the border area of MI hearts at 4 days after MI. Twenty fields of 200 μm × 200 μm for the border area were analyzed for each mouse at a magnification of × 400/high-power field (HPF). The inflammatory cells in the border area of MI hearts were identified with anti-Ly6G antibody (granulocytes), anti-Mac3antibody (macrophages), and anti-CD3 antibody (T-lymphocytes; BD PharMingen, San Diego, CA) at 4 day after MI. Furthermore, we performed an additional experiment to analyze apoptotic cells by TUNEL method at Days 1, 4, and 7 after MI (Control, n=15; Post-G, n=15). TUNEL assay was performed with an apoptosis detection kit (Takara Syuzo, Kyoto, Japan) as described previously (11). Furthermore, we examined double-immunohistochemical analysis with anti-von Willebrand factor antibody (DAKO, A/S, Denmark) to identify apoptotic endothelial cells.

Bone marrow transplantation

BM cells of GFP transgenic mice (12) were transplanted into C57BL/6 male mice as described previously (13). Flow cytometry analysis revealed that the BM chimerism was more than 70%. BM cells were identified by immunostaining with anti-GFP antibody (Medical and Biological Laboratories. CO., Nagoya, Japan) as described previously (14).

Statistics

All data are presented as mean ± SD. Multiple group comparison was performed by one-way ANOVA followed by the Bonferroni procedure for comparison of means. Survival rates of mice were analyzed by Kaplan-Meier method. Probability values less than 0.05 were considered to be statistically significant.

RESULTS

Mortality

The survival rates of mice at 14 days after MI were significantly higher in the three cytokine treatment groups with G-CSF (pre-GS, 63%; post-GS, 80%; and post-G, 70%) than in the control group (23%, P<0.05) and the post-S group (43%, P<0.05) in Kaplan-Meier method (Fig. 1*B*). There was no significant difference in the survival rates between pre- and post-treatment with

cytokines and between the combination treatment with G-CSF and SCF, and the treatment with G-CSF alone.

Physiological analysis

In the present study, we examined cardiac function by echocardiogram a few days before grouping. The mice with normal cardiac function were used in this study. Therefore, the degree of baseline LV function in mouse was equal among the groups before entry for the study. At 2 weeks after MI, there was no significant difference in the heart rate among all the groups (data not shown). LVP was higher in the three cytokine treatment groups with G-CSF than in the control group and the post-S group (Table 1). LVEDP was elevated in the control group and the post-S group but not the three treatment groups with G-CSF (Table 1). Furthermore, dP/dt and –dP/dt were larger in the three treatment groups with G-CSF than in control group and post-S group (Table 1). There was no significant difference in these parameters among the three cytokine treatment groups with G-CSF. These results suggest that all the three cytokine treatments with G-CSF improve systolic and diastolic functions of LV after MI.

Histological analysis

After MI, LV free wall was very thin and LV cavity was markedly expanded in control group and post-S group but LV wall thickness and LV cavity were preserved normal in the three treatment groups with G-CSF (Fig. 2*A*). Although the percentage of fibrotic area to the whole LV area was similar among cytokine treatment groups and the control group (control, 38.9 ± 9.7%; pre-GS, 35.2 ± 3.4%; post-GS, 33.1 ± 11.0%; post-G, 32.0. ± 5.4%; post-S, 32.8 ± 4.2%; Fig. 2*B*), the wall thickness was greater in the three cytokine treatment groups with G-CSF (sham, 1.14 ± 0.06 mm; pre-GS, 0.52 ± 0.14 mm; post-GS, 0.57 ± 0.20 mm; post-G, 0.53. ± 0.16 mm) than in control group (0.23 ± 0.07 mm) and post-S group (0.31 ± 0.08 mm; Fig. 2*C*). There was no significant difference in the wall thickness among all the three treatment groups with G-CSF.

Infiltration of white blood cells

G-CSF has been reported to increase the number of peripheral granulocytes (15). In this study, the number of granulocytes at 4 days after MI was higher in the three treatment groups (pre-GS, 12886 ± 773/mm^3; post-GS, 13912 ± 1447/mm^3; and post-G, 14318 ± 2736/mm^3) than in the control group (3056 ± 959/mm^3, $P<0.05$), but there was no histological evidence suggesting immunoreactions in all organs examined in our animal model. We next examined whether the number of infiltrated cells into the heart was also increased and, if so, what kinds of cells infiltrated into the heart. Immunohistochemical analysis using specific antibodies revealed that there was infiltration of granulocytes, macrophages, and T lymphocytes in the hearts of 4 days after MI. More granulocytes were observed in the hearts of the three treatment groups with G-CSF (pre-GS, 56.8 ± 15.0/10^{3}cells; post-GS, 62.2 ± 14.0/10^{3}cells; post-G, 58.7 ± 15.0/10^{3}cells) than in control group (32.1 ± 5.0/10^{3}cells, $P<0.05$) at 4 days after MI (Fig. 3*A*, *B*). There was no significant difference in the number of macrophages (Fig. 3*C*, *D*) and T lymphocytes (Fig. 3*E* and *F*) among the three treatment groups with G-CSF and control group.

Mobilization of BM cells

We next examined whether BM cells were infiltrated into the heart by using the mice whose BM was replaced by that of GFP-expressing mice. Because it was difficult to discriminate

GFP-expressing BM cells from other types of cells because of autofluorescence of MI hearts (Fig. 4*A*), we identified BM-derived cells by using anti-GFP antibody. Many GFP-positive cells were recognized in the border area of all the three treatment groups but not the control group (Fig. 4*B*). Most of GFP-positive cells were infiltrated blood cells (arrows in Fig. 4*B*), and some GFP-positive cells were observed at capillary walls (Fig. 4*C*). There were few GFP-positive cardiomyocytes (less than 0.01%) in the border area as well as in the infarcted area and the remote area. Therefore, we next compared the number of vessels in the border area. The number of capillaries in the border area after MI was much greater in all the three treatment groups (pre-GS, 8.0 ± 2.3/HPF; post-GS, 7.8 ± 1.7/HPF; post-G, 6.2 ± 1.9/HPF) than in the control group (2.0 ± 0.82/HPF, $P<0.05$; Fig. 4*D* and *E*).

Apoptotic cells in border area

We examined apoptotic cell death in the border area after MI. The number of TUNEL-positive cells in the border area of infarcted heart at Day 4 after MI was significantly smaller in the three treatment groups (pre-GS, 13.3 ± 3.2/10^3cells; post-GS, 10.8 ± 1.5/10^3cells; post-G, 12.8 ± 1.0/10^3cells, not significant among three groups) than in control group (30.7 ± 3.7/10^3cells, $P<0.05$; Fig. 4*F* and *G*). At Days 1 and 4, the number of TUNEL-positive cells was significantly smaller in Post-G group (Day 1, 73.8 ± 11.4/10^3cells; Day 4, 12.8 ± 1.0/10^3cells; Day 7, 4.7 ± 2.0/10^3cells) than in control group (Day 1, 116.0 ± 17.1/10^3cells; Day 4, 30.7 ± 3.7/10^3cells; Day 7, 4.2 ± 1.9/10^3cells, $P<0.05$; Fig. 5*A*). Furthermore, we examined double-immunohistochemical analysis to identify the cell type of apoptotic cells. We observed very few apoptotic cardiomyocytes at all the time points. The percentage of von Willebrand factor-positive cells in TUNEL-positive cells was significantly smaller in the Post-G group (Day 1, 0.8 ± 0.5%) than in control group (Day 1, 5.5 ± 1.5 %, $P<0.05$; Fig. 5*B*).

DISCUSSION

Because LV remodeling after MI determines subsequent cardiac function and prognosis, the inhibition of LV remodeling is clinically very important (1). After MI, many cardiomyocytes undergo cell death by the mechanisms of necrosis and apoptosis in the infarcted area, which is then replaced by fibrous tissue. The infarcted area is gradually extended by the subsequent death of cardiomyocytes and vascular cells in the border area and expanded by abnormal wall tension (2). Myocardial ischemia plays a critical role in the cardiomyocyte death in the border area after MI and thus greatly affects LV remodeling. It has been reported that a subset of BMSCs differentiates into cardiomyocytes when injected into peri-infarcted area, which results in regeneration of infarcted heart (3). Moreover, it has been reported that pretreatment with G-CSF and SCF attenuates LV remodeling after MI (4). Although these results suggest that the cytokine treatment is beneficial to prevent LV remodeling, the cytokine treatment was started before MI and thus this protocol cannot be applied to humans. Furthermore, the molecular mechanism of how the cytokine treatment repairs the infarcted heart is not fully understood. In the present study, 1) cytokine treatments started after MI were as effective as the pretreatment; 2) there was no significant difference in all parameters, including fibrotic area, cardiac function, and survival rate between the treatment with G-CSF alone and the combination treatment with G-CSF and SCF; 3) more capillaries were observed in the border area of the treatment groups with G-CSF compared with control group and SCF alone group, and the number of apoptotic cells was smaller in the three cytokine treatment groups with G-CSF than in control group.

It is very important to determine whether the combination therapy of G-CSF and SCF has additive effects on LV remodeling and cardiac function. Although it was reported that the combined treatment with G-CSF and SCF synergistically increased mobilization of BMSCs, it remains unknown whether the combined treatment also has synergistic effects on MI heart. Therefore, we compared the effects of G-CSF alone or SCF alone with those of combination treatment on LV remodeling and cardiac function after MI. Although the treatment with G-CSF alone showed effects similar to the combination treatment, the treatment with SCF alone could neither prevent LV remodeling nor improve survival rate after MI. It was previously reported that continuous treatment with SCF alone failed to induce any detectable change in the number of WBC throughout first 5 days and that a transient increase in WBC was increased at Day 7 after treatment in normal mice (16). Treatment with G-CSF alone increased the number of WBC at Day 4 after treatment. The different ability of BMSC mobilization between G-CSF and SCF may cause the different effects on LV remodeling after MI. These results suggest that G-CSF treatment started after MI is as beneficial as the pretreatment or the combination treatment with G-CSF and SCF to prevention of LV remodeling.

It has been reported that G-CSF induces the mobilization of BMSCs from BM into the peripheral blood circulation (17). There were more capillaries in the border area of all the cytokine treatment groups with G-CSF than in control group after MI, and a part of the cells constituting the capillary wall were derived from BM cells. There were few GFP-positive cardiomyocytes in the hearts in spite of the cytokine therapy. We think two possible mechanisms by which the cytokine therapy has beneficial effects on MI heart. One mechanism is that the cytokine therapy mobilizes BMSCs into MI heart and induces angiogenesis. Several lines of evidence suggest that BMSCs injected into myocardium induce angiogenesis (18, 19). Another mechanism is that the number of apoptotic endothelial cells is decreased by the cytokine therapy. The number of both von Willebrand factor and TUNEL-positive cells was significantly smaller in the Post-G group than in the control group. These mechanisms may result in an increase in capillary density leading to a decrease in apoptosis of cardiac myocytes in the border area. Recently, we observed that G-CSF induced activation of Akt, which has been reported to play an important role in cell survival and angiogenesis (20), in the border area after MI in swine (unpublished data). These results suggest that an increase in Akt activity by G-CSF may be also associated with an increase in the number of capillary vessels and a decrease in the number of apoptotic cells in the border area, resulting in better myocardial perfusion and less remodeling in the border area. Moreover, we recently examined whether G-CSF influences expression level of an angiogenic growth factor, vascular endothelial growth factor (VEGF; 21), after MI in swine. The expression of VEGF protein in the border area was increased in G-CSF-treated group than in the control group after MI (unpublished data). Further studies are needed to clarify what kinds of growth factors and cytokines are involved in angiogenic effects of the cytokine therapy in mouse MI model, and it also remains to be determined which cells (e.g., hematopoietic stem cells, mesenchymal stem cells, and endothelial progenitor cells) become vascular cells and whether neovascularization is a major mechanism for G-CSF-induced prevention of LV remodeling after MI.

ACKNOWLEDGMENTS

We thank to R. Kobayashi, E. Fujita, M. Watanabe, M. Iida, and A. Ohkubo for technical assistance. This work was supported by Takeda Medical Research Foundation, Uehara Memorial Foundation, Grant-in-Aid of The Japan Medical Association, The Kato Memorial Trust for Nambyo Research and Takeda Science Foundation.

REFERENCES

1. Pfeffer, M. A., and Braunwald, E. (1990) Ventricular remodeling after myocardial infarction. Experimental observations and clinical implications. *Circulation* **81,** 1161–1172

2. Krijnen, P. A., Nijmeijer, R., Meijer, C. J., Visser, C. A., Hack, C. E., and Niessen, H. W. (2002) Apoptosis in myocardial ischaemia and infarction. *J. Clin. Pathol.* **55,** 801–811

3. Orlic, D., Kajstura, J., Chimenti, S., Jakoniuk, I., Anderson, S. M., Li, B., Pickel, J., McKay, R., Nadal-Ginard, B., Bodine, D. M., et al. (2001) Bone marrow cells regenerate infarcted myocardium. *Nature* **410,** 701–705

4. Orlic, D., Kajstura, J., Chimenti, S., Limana, F., Jakoniuk, I., Quaini, F., Nadal-Ginard, B., Bodine, D. M., Leri, A., and Anversa, P. (2001) Mobilized bone marrow cells repair the infarcted heart, improving function and survival. *Proc. Natl. Acad. Sci. USA* **98,** 10344–10349

5. Davani, S., Marandin, A., Mersin, N., Royer, B., Kantelip, B., Herve, P., Etievent, J. P., and Kantelip, J. P. (2003) Mesenchymal progenitor cells differentiate into an endothelial phenotype, enhance vascular density, and improve heart function in a rat cellular cardiomyoplasty model. *Circulation* **108,** 253–258

6. Mangi, A. A., Noiseux, N., Kong, D., He, H., Rezvani, M., Ingwall, J. S., and Dzau, V. (2003) Mesenchymal stem cells modified with Akt prevent remodeling and restore performance of infarcted hearts. *Nat. Med.* **9,** 1195–1201

7. Harada, K., Sugaya, T., Murakami, K., Yazaki, Y., and Komuro, I. (1999) Angiotensin II type 1A receptor knockout mice display less left ventricular remodeling and improved survival after myocardial infarction. *Circulation* **100,** 2093–2099

8. Takimoto, E., Yao, A., Toko, H., Takano, H., Shimoyama, M., Sonoda, M., Wakimoto, K., Takahashi, T., Akazawa, H., Mizukami, M., et al. (2002) Sodium calcium exchanger plays a key role in alteration of cardiac function in response to pressure overload. *FASEB J.* **16,** 373–378

9. Li, Y., Takemura, G., Kosai, K., Yuge, K., Nagano, S., Esaki, M., Goto, K., Takahashi, T., Hayakawa, K., Koda, M., et al. (2003) Postinfarction Treatment With an Adenoviral Vector Expressing Hepatocyte Growth Factor Relieves Chronic Left Ventricular Remodeling and Dysfunction in Mice. *Circulation* **107,** 2499–2506

10. Toko, H., Zhu, W., Takimoto, E., Shiojima, I., Hiroi, Y., Zou, Y., Oka, T., Akazawa, H., Mizukami, M., Sakamoto, M., et al. (2002) Csx/Nkx2-5 is required for homeostasis and survival of cardiac myocytes in the adult heart. *J. Biol. Chem.* **277,** 24735–24743

11. Hadjantonakis, A. K., and Nagy, A. (2001) The color of mice: in the light of GFP-variant reporters. *Histochem. Cell Biol.* **115,** 49–58

12. Yoder, M. C., Hiatt, K., Dutt, P., Mukherjee, P., Bodine, D. M., and Orlic, D. (1997) Characterization of definitive lymphohematopoietic stem cells in the day 9 murine yolk sac. *Immunity* **7,** 335–344

13. Krause, D. S., Ito, T., Fackler, M. J., Smith, O. M., Collector, M. I., Sharkis, S. J., and May, W. S. (1994) Characterization of murine CD34, a marker for hematopoietic progenitor and stem cells. *Blood* **84,** 691–701

14. To, L. B., Haylock, D. N., Simmons, P. J., and Juttner, C. A. (1997) The biology and clinical uses of blood stem cells. *Blood* **89,** 2233–2258

15. Clark, S. C., and Kamen, R. (1987) The human hematopoietic colony-stimulating factors. *Science* **236,** 1229–1237

16. Molineux, G., Migdalska, A., Szmitkowski, M., Zsebo, K., and Dexter, T. M. (1991) The effects on hematopoiesis of recombinant stem cell factor (ligand for c-kit) administered in vivo to mice either alone or in combination with granulocyte colony-stimulating factor. *Blood* **78,** 961–966

17. Tanaka, J., Miyake, T., Shimizu, T., Wakayana, T., Tsumori, M., Koshimura, K., Murakami, Y., and Kato, Y. (2002) Effect of continuous subcutaneous administration of a low dose of G-CSF on stem cell mobilization in healthy donors: a feasibility study. *Int. J. Hematol.* **75,** 489–492

18. Kamihata, H., Matsubara, H., Nishiue, T., Fujiyama, S., Tsutsumi, Y., Ozono, R., Masaki, H., Mori, Y., Iba, O., Tateishi, E., et al. (2001) Implantation of Bone Marrow Mononuclear Cells Into Ischemic Myocardium Enhances Collateral Perfusion and Regional Function via Side Supply of Angioblasts, Angiogenic Ligands, and Cytokines. *Circulation* **104,** 1046–1052

19. Strauer, B. E., Brehm, M., Zeus, T., Köstering, M., Hernandez, A., Sorg, V. R., Kögler, G., and Wernet, P. (2002) Repair of infarcted myocardium by autologous intracoronary mononuclear bone marrow cell transplantation in humans. *Circulation.* **106,** 1913–1918

20. Koc, O. N., and Gerson, S. L. (2003) Akt helps stem cells heal the heart. *Nat. Med.* **9,** 1109–1110

21. Kupatt, C., Hinkel, R., Vachenauer, R., Horstkotte, J., Raake, P., Sandner, T., Kreuzpointner, R., Muller, F., Dimmeler, S., Feron, O., et al. (2003) VEGF165 transfection decreases postischemic NF-kappa B-dependent myocardial reperfusion injury in vivo: role of eNOS phosphorylation. *FASEB J.* **17,** 705–707

Received August 19, 2003; accepted January 20, 2004.

Table 1

Hemodynamic parameter after MI

	Sham (n=5)	Control (n=5)	Pre-GS (n=10)	Post-GS (n=16)	Post-G (n=14)	Post-S (n=9)
LVP (mmHg)	103.1±13.9	61.8±11.7	87.3±16.1*	89.9±17.5*	85.7±6.7*	63.3±5.5
LVEDP (mmHg)	2.0±0.8	13.3±6.8	4.1±2.5*	3.3±3.3*	4.2±2.6*	12.4±2.5
dP/dt (mmHg/s)	6034±302	2048±558	2860±567*	3241±710*	2558±373*	2106±466
–dP/dt (mmHg/s)	5805±364	2018±459	2778±567*	3169±703*	2598±371*	2011±479

LVP, left ventricular systolic pressure; LVEDP, left ventricular end-diastolic pressure; dP/dt and –dP/dt, positive and negative first derivatives for maximal rates of left ventricular pressure development.
Values are mean ± SD. *P < 0.05 vs. Control group.

Fig. 1

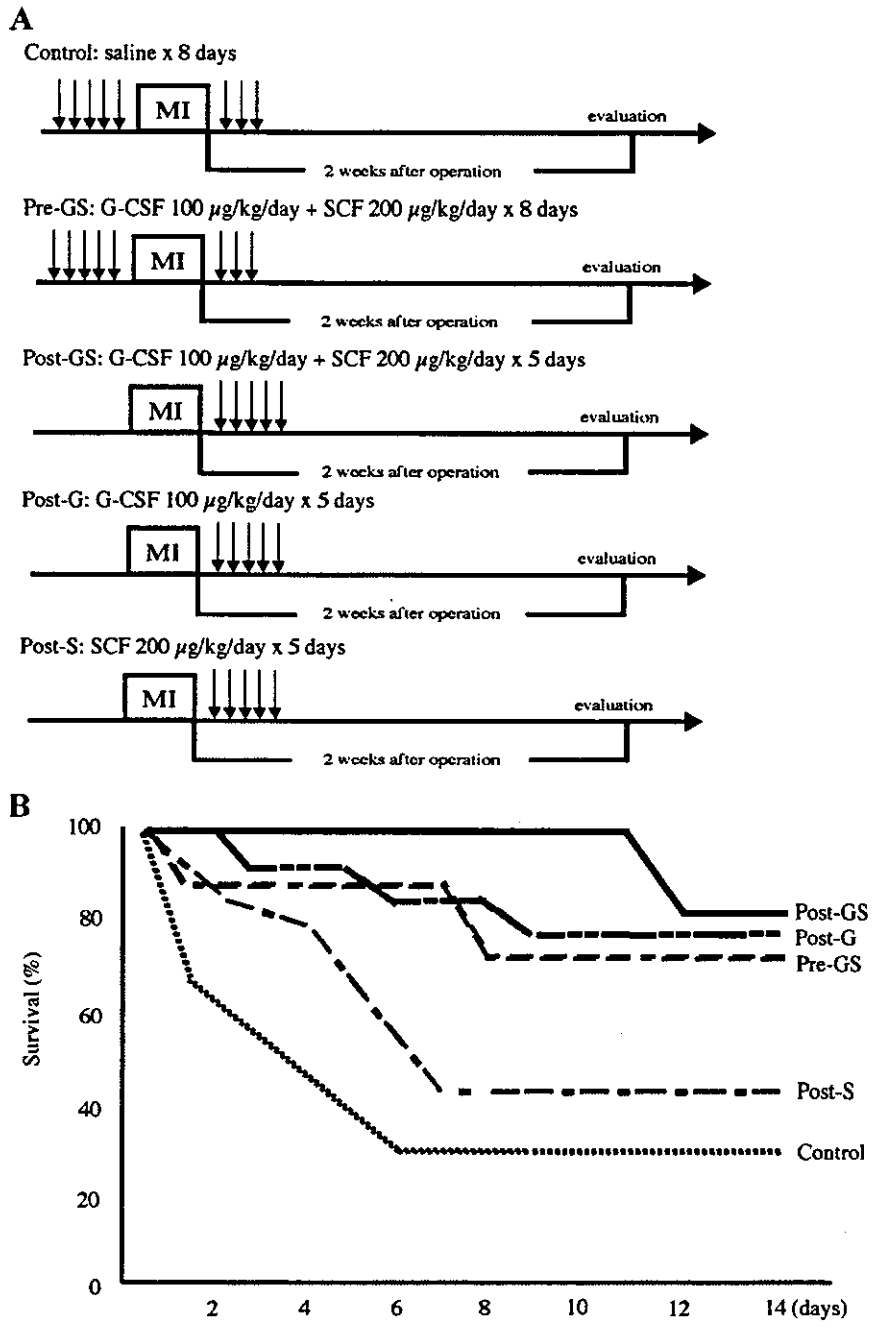

Figure 1. Protocol of the cytokine treatment and survival rate. ***A)*** Mice in pretreatment group (Pre-GS) were injected subcutaneously (s.c.) with SCF (200 μg/kg/day) and G-CSF (100 μg/kg/day) from 5 days before MI until 3 days after MI (n=16). Mice in post-treatment groups were injected s.c. with G-CSF alone (Post-G; n=20), SCF alone (Post-S; n=21), or SCF and G-CSF once a day for 5 days after MI (Post-GS; n=20). Mice in control group (Control) were injected with saline for 8 days before and after MI (n=22). ***B)*** Survival rates of mice at 14 days were higher in 3 treatment groups with G-CSF than in control group in Kaplan-Meier method.

Fig. 2

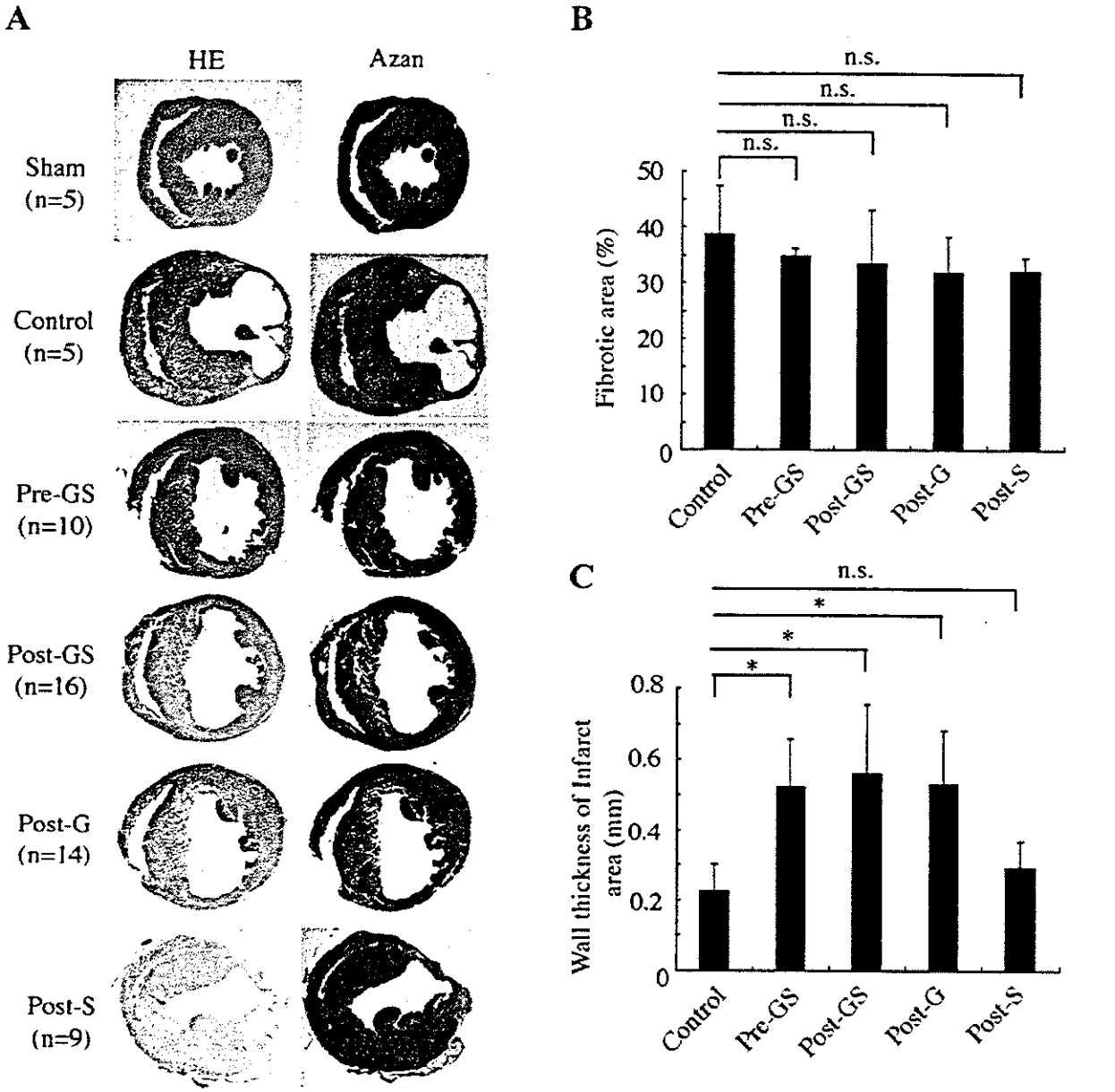

Figure 2. Morphological analysis. We examined hemodynamic parameters of the survived mice (Sham, n=5; Control, n=5; Pre-GS, n=10; Post-GS, n=16; Post-G, n=14; Post-S, n=9) at 2 weeks after MI by cardiac catheterization and subsequently performed histological analysis. ***A***) Light microscopic analysis in hematoxylin-eosin (HE) staining and Azan-Mallory staining. LV free wall was thinner in heart of control group and Post-S group than in heart of Post-G, Post-GS, and Pre-GS groups (HE: left panel). Infarct area was replaced completely by fibrotic tissue in control group, while remained myocardium was observed in the hearts of all the treatment groups with G-CSF (Azan: right panel). ***B***) Fibrotic area in the whole LV area. There was no significant difference in the percentages of fibrotic area among the treatment groups and control group (n.s., not significant.). ***C***) Wall thickness of infarct area was thinner in hearts of control group and Post-S group than in hearts of Post-G, Post-GS, and Pre-GS groups (*P<0.05).

Fig. 3

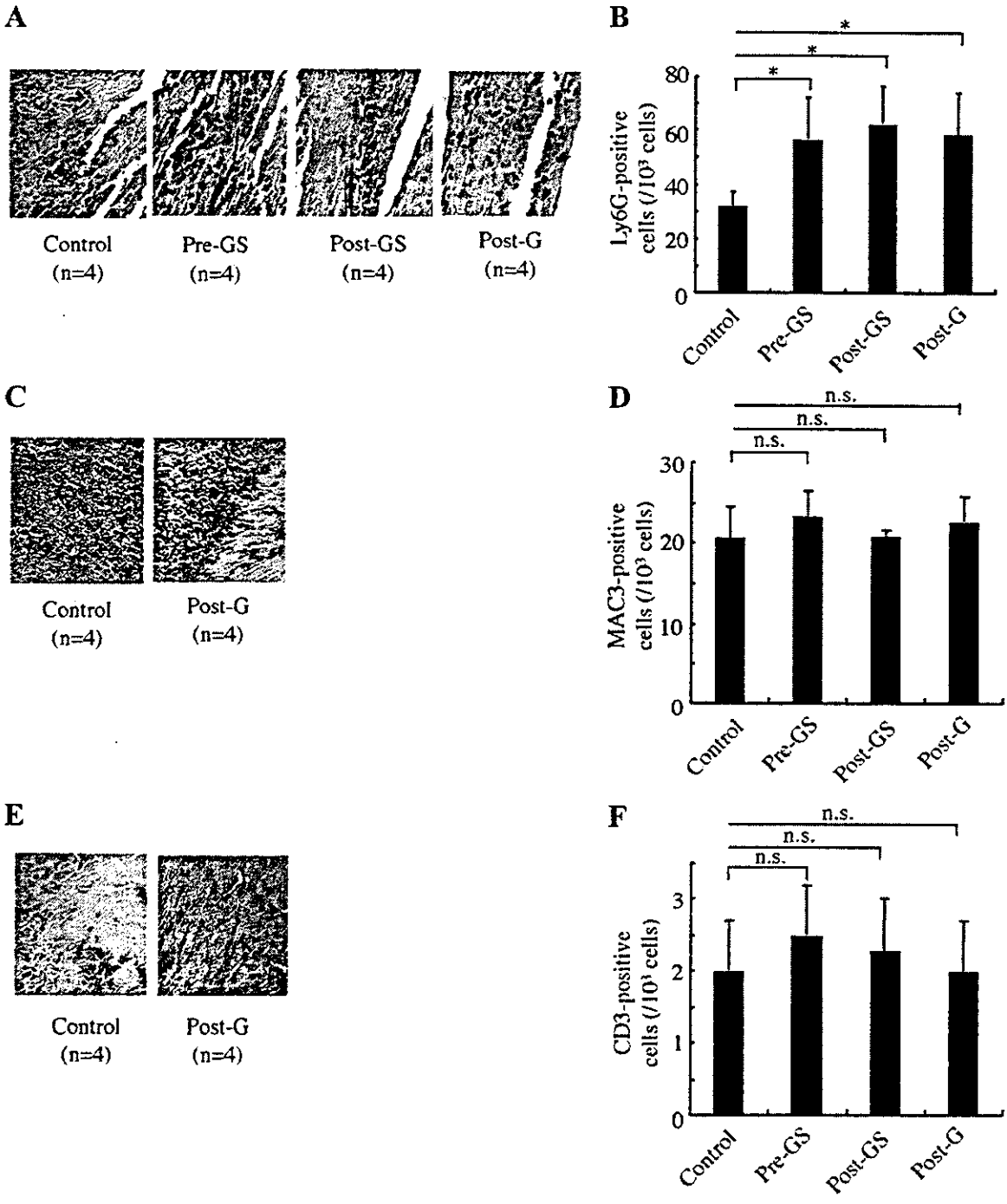

Figure 3. Inflammatory cells in the heart. *A, B)* The number of Ly6G-positive cells (granulocytes) at the border area of infarcted heart was greater in the three treatment groups than in control group (*$P<0.05$) at 4 days after MI. There was no significant difference in the number of MAC3-positive cells (macrophages; *C, D*) and CD3-positive cells (T-lymphocytes; *E, F*) among the three treatment groups and control group.